Hygrothermal component models for greenhouse simulation in TRNSYS

Clémence Lavigueur[1], Michaël Kummert[1]
[1]Polytechnique Montréal, Montréal, Canada

Abstract

Greenhouse production is a viable solution to enhance food self-reliance, but the associated energy use for heating, dehumidification and artificial lighting is significant in Canadian climates. Building performance simulation tools can be used to simulate greenhouses and optimize their design and operation, but building models typically simplify or neglect key processes in the hygrothermal balance of a thermal zone in the presence of plants: convection, radiation, and evapotranspiration from plants is more complex than moisture gains from occupants or equipment, and condensation plays a significant role in moisture removal. This paper proposes two models that represent these processes more accurately and that can be combined with the existing dynamic building model implemented in TRNSYS. Both models are compared to experimental data from original measurements or from the literature.

Introduction

The recent COVID-19 pandemic has highlighted the risks of food supply chains relying on international markets. The Canadian food sector is largely self-reliant for some categories such as meat but relies heavily on imports for fresh vegetables. Governments and citizens have realized the need to strive for self-sufficiency. Greenhouses will play a key role in reaching that objective, and Quebec's government has for example announced a strategy to double greenhouse production of fruits and vegetables by 2025 (Gouvernement du Québec, 2020).

Greenhouses must be heated and dehumidified to ensure production all year round, and they often use artificial lighting during darker periods, which results in high energy costs. Reducing the financial burden and environmental impact of energy use is one of the main objectives of research addressing greenhouses design and operation, which requires suitable models (Pelletier and Godbout, 2017; Bouthillette Parizeau, 2021).

Several complete greenhouse models have been proposed in the literature. They address the plants hygrothermal balance, the building thermal model, and detailed plant growth models allowing to quantify food production (Ward and Choudhary, 2014; Mohammadi, Ranjbar and Ajabshirchi, 2021). But these models require detailed knowledge of the plants and growth cycles and implement simplified (often 1-D) models for the building thermal balance.

Building performance simulation (BPS) models are a natural choice to assess the energy performance of greenhouses, because they implement all the required energy balances. But they typically lack models to represent the plants interactions with their environment. Internal (or casual) moisture and sensible gains are usually accounted for using predefined values and schedules. This is an acceptable assumption for typical buildings but not for greenhouses, where the indoor conditions typically vary within a larger range, and the heat and moisture exchanges with the plants vary with indoor conditions. BPS models also typically treat condensation as a process that should not be occurring, e.g. by raising a flag to indicate the presence of surface temperatures below the indoor dewpoint. Greenhouses present a relatively high indoor humidity and large glazing surfaces with low indoor surface temperature during cold periods, so the impact of condensation on the zone moisture balance must be quantified.

Our research goal is to assess design and operation scenarios for greenhouses integrated in urban energy systems. TRNSYS was selected because it offers a detailed dynamic building model, as well as components required to model heating and ventilation systems and detailed ground heat transfer. Our objective in this paper is to develop two new component models to account for condensation and for the hygrothermal exchanges with plants, striking a balance between accuracy and the complexity of the models and their required input data (or parameters).

The first two sections in the paper present the condensation component model and the plant component model, comparing their results to experimental data from original measurements or the literature. The third section illustrates the results of a global greenhouse model combining the proposed models to existing components in TRNSYS.

Condensation model

Condensation is associated with serious risks such as mould, so it should not normally happen in standard buildings. This explains that little attention is paid to condensation in BPS tools, apart from flagging surface temperatures that are below the room temperature dewpoint. In TRNSYS (Klein *et al.*, 2021), the dynamic building component model, known as Type 56, performs a moisture balance taking into account ventilation, infiltration, and latent gains, in addition to moisture addition/removal by idealized heating and cooling systems. Condensation is not quantified, and as of version 18.4, Type 56 also keeps increasing the humidity ratio if moisture is added beyond 100 % relative humidity in a thermal zone, which can result in error accumulation for high-humidity environments. For this reason, we decided to create a component model (TRNSYS Type) that should be connected to the building Type 56 to model condensation.

Model assumptions

Condensation takes place when a vapor is cooled below its saturation temperature, which for humid air is equivalent to say that the humid air mixture is cooled below its dewpoint temperature. When condensation occurs on a cold surface, the condensed water is collected on the surface (as droplets, in our case), and the latent heat of the vapor is released to the surface. Th extraction of water vapor from the air on a surface can be described with the following equation:

$$\dot{m} = \frac{h_{tot} \cdot (T_{dp} - T_s)}{\mathcal{L}} \qquad (1)$$

$\dot{m}$ is the condensation rate, h_{tot} is the overall heat transfer coefficient, T_{dp} is the dew point temperature, T_s is the surface temperature, and $\mathcal{L}$ is the latent heat of vaporization of water. The overall heat transfer coefficient is calculated with the Griffith (1983) correlation, which was established for a copper surface and pure steam:

$$h_{\text{tot,u}} = \begin{cases} 51104 + 2044\ T_{dp} & \text{if} \quad T_{dp} < 100\ °C \\ 255510 & \text{if} \quad T_{dp} > 100\ °C \end{cases} \qquad (2)$$

Where T_{dp} is the dewpoint temperature in °C, and $h_{tot,u}$ is in W m^{-2} K^{-1} (the "u" denotes that the coefficient is uncorrected). Griffith (1983) proposes curves to correct h_{tot} for different materials than copper and in the presence of non-condensing gases (such as for humid air). The conditions for glass or plastic surfaces and typical moisture concentrations in humid air are at the extreme limits of the curves provided for the correction factors, which results in a large uncertainty on the corrected h_{tot}:

$$h_{tot} = c \cdot\ h_{tot,u} \ \text{ with } c \approx 0.0001 \text{ to } 0.0005 \qquad (3)$$

The heat transferred to the surface $\dot{Q}_s$ can be calculated as:

$$\dot{Q}_s = \dot{m} \cdot \mathcal{L} \qquad (4)$$

The heat released by condensation is assumed to be partially absorbed at the internal surface and partially released within the zone air volume. It is distributed between a "gain" and a "wall gain" in Type 56. The water vapor removed from the room is implemented as a negative humidity gain.

Figure 1 shows how the developed component model interacts with the building model in TRNSYS.

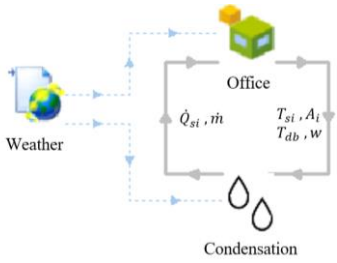

Figure 1: Data exchange between the developed component model for condensation and TRNSYS Type 56

For each surface i, $\dot{Q}_{s,i}$ is the heat transferred by condensation on the surface, $T_{s,i}$ is the internal surface temperature, and A_i is the surface area. T_{db} and w are respectively the dry bulb temperature and the humidity ratio in the room. The connection to the weather component gives the atmospheric pressure for psychrometric calculations.

Comparison with published experimental data

The condensation model was compared to the experimental data presented in Nguyen *et al.* (2019) for a test room where condensation is induced on a large window. Internal surface temperatures are controlled and maintained at relatively constant values, and moisture is added to the room through ventilation. The test room is represented in Figure 2.

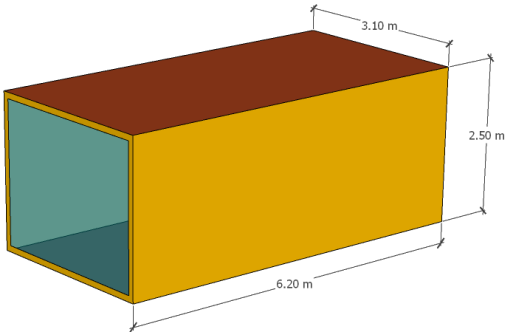

Figure 2: Test room used in Nguyen et al. (2019)

Inside surface temperatures are maintained at constant values, as shown in Table 1. The ventilation flowrate is constant, but its relative humidity is increased abruptly at the beginning of the test, as shown in Table 2.

The test room was modelled in TRNSYS and the ventilation supply conditions were imposed to the model. The mass flowrate of water condensed on the cool window is compared to experimental values in Figure 3.

Table 1: Indoor surface temperatures (kept constant)

Surface	**Roof**	**West**	**Floor**	**East**	**North**	**South (Window)**
Temp. [°C]	21.4	21.2	21.1	21.1	21.3	15.3

Table 2: Ventilation supply conditions in the experiment

	Flow rate [m³/h]	Temperature [°C]	Humidity ratio [kg/kg]
Before test	150	28.0	0.00901
During test	150	28.1	0.01407

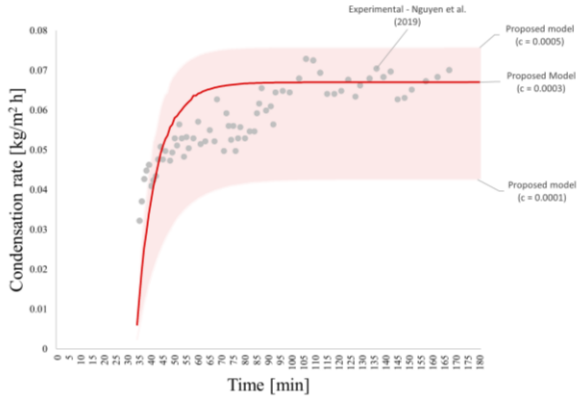

Figure 3: Comparison between the experimental condensation flowrate in Nguyen et al. (2019) and the developed component model for surface condensation

The modelled condensation flowrate is more stable than the experimental flowrate, which can be attributed to small variation in the experimental conditions which are acknowledged in Nguyen *et al.* (2019), while the simulation uses the constant boundary temperatures shown in Table 1. The condensation flowrate calculated with c in (3) varying between 0.0001 and 0.0005 seems to provide a reasonable approximation of the steady-state value reached during the last part of the test, given the large uncertainties in heat transfer coefficients and the large variations in experimentally measured dropwise condensation. The model is implemented with a value of $c = 0.0003$, which corresponds to the middle of the estimated range and delivers a mean bias error of 0.0002 kg m^{-2} h^{-1} over the test duration, which corresponds to 0.3 % of the steady state value over the last hour of the test. Additional comparisons with experimental data would be necessary to recommend a more accurate value.

Plant model

Most plant models are based on the seminal work by Penman and Monteith, who formulated the steady state heat balance and the evaporation model for a water or soil surface, and then adapted it to a leaf or vegetation canopy (see e.g. Monteith and Unsworth, 2013 for a historical perspective). The heat balance (equation (5) below) and the equation for vapor diffusion (equation (15) below) are fundamental equations, so all "plant models" rely on these equations (or some empirical approximation of the vapor diffusion). Models differ in the systems they consider (soil, canopy, leaf), simplifying assumptions, and solving methods. Sometimes, a "plant model" described in the literature also includes – or in fact is only differentiated by – specific values or relationships for key parameters in the model, such as the leaf stomatal resistance (which is introduced below). This has resulted in a large number of "plant models", some of which have been implemented in BPS tools. Kokogiannatis & Cooper (2015) implemented a plant model derived from the Penman-Monteith equation in ESP-r, neglecting longwave radiation. Talbot & Monfet (Talbot and Monfet, 2020) implemented in TRNSYS an algorithm proposed by Graamans et al. (2017). The algorithm uses the Penman-Monteith linearization, which was introduced to be able to solve the balance without iterations, but the paper still presents an iterative solution procedure for the linearized problem. Longwave radiation is neglected, and some parameters (and their assumed variation) are applicable to lettuce production in indoor "plant factories" under 100 % artificial lighting. Our objectives in developing the model described below are to represent longwave radiation in a typical greenhouse and to implement generic and flexible relationships for model parameters related to plant species, while describing in detail the reference area used to parametrize the model.

Model assumptions: steady state hygrothermal balance

The basis for our approach is known as the "big leaf" model, also known as the Penman-Monteith model (Monteith, 1965). A good overview of the different processes involved is provided in Monteith & Unsworth (2013). The basic assumption of the model is that the plants can be reduced to an equivalent 1-D "big leaf" that absorbs shortwave radiation, exchanges sensible heat through convection and longwave radiation, and loses water vapor by transpiration.

The steady-state heat balance of plants can be described as:

$$\dot{q}_{rad,sw} + \dot{q}_{met} = \dot{q}_{conv} + \dot{q}_{rad,lw} + \dot{q}_{cond} + \dot{q}_{lat} \qquad (5)$$

On the left side are two positive terms (energy gains): $\dot{q}_{rad,sw}$ is the absorbed shortwave radiation (from the sun and artificial lighting), $\dot{q}_{met}$ is the net gain from metabolism. On the right side are terms that typically correspond to energy losses, but can be negative (i.e. represent gains) depending on environmental conditions: sensible heat losses by convection ($\dot{q}_{conv}$), longwave radiation ($\dot{q}_{rad,lw}$), and conduction ($\dot{q}_{cond}$); latent heat losses by transpiration ($\dot{q}_{lat}$).

Most models neglect the conduction heat loss and the heat gain from metabolism, which represent small energy transfers (Monteith and Unsworth, 2013; Ward *et al.*, 2015; Graamans *et al.*, 2017; Talbot and Monfet, 2020; Wei, Nourozi and Chen, 2021). With those assumptions, the steady-state plant heat balance becomes:

$$\dot{q}_{rad,sw} = \dot{q}_{conv} + \dot{q}_{rad,lw} + \dot{q}_{lat} \qquad (6)$$

It should be noted that all heat fluxes are expressed per unit of surface (W/m²). In plants, the surface area receiving solar

radiation (upper face of unshaded leaves) is not equal to the surface area losing heat by convection (both faces of all leaves), so care must be taken when expressing the heat balance. The reference area used for the heat balance is the cultivated area, i.e. the useful greenhouse floor area, not counting large circulation areas, technical rooms, etc.

Shortwave radiation

If we assume that the shortwave radiation from the sun or artificial lighting comes from the top of the greenhouse, a reasonable estimation of the net absorbed radiation is:

$$\dot{q}_{rad,sw} = G \cdot \tau_s \cdot \alpha_s \cdot CAC \qquad (7)$$

Where G is the horizontal solar radiation (or radiation from artificial lighting), τ_s is the overall transmittance of the greenhouse cover (or 1 in the case of artificial lighting), α_s is the absorptance of the plant surface, and CAC is the ratio between the horizontal projection of the leaf area and the cultivated area, which is called the *Cultivation Area Cover*. CAC is introduced because the heat balance is expressed per unit of cultivated area, but the area of leaves that effectively absorbs shortwave radiation only represents a fraction (CAC) – in other words, CAC is the number of (horizontally projected) square meters of leaf absorbing solar radiation per square meter of cultivated area (useful greenhouse area).

Convection

The convection heat losses from the plants is related to the leaf surface temperature (T_s) and the dry bulb temperature of the air (T_a):

$$\dot{q}_{conv} = h_{conv} \cdot (T_s - T_a) \qquad (8)$$

In agricultural sciences, the convection coefficient h_{conv} is usually expressed as (Monteith and Unsworth, 2013):

$$h_{conv} = \frac{\rho \cdot c_p}{r_{conv}} \qquad (9)$$

Where ρ (kg/m³) and c_p (J kg^{-1} K^{-1}) are the density and specific heat of the moist air, and r_{conv} is the resistance to convective heat transfer (s m^{-1}). The convective heat transfer is then:

$$\dot{q}_{conv} = \frac{\rho \cdot c_p}{r_{conv}} \cdot (T_s - T_a) \qquad (10)$$

The resistance r_{conv} can be expressed as a function of the Nusselt number, which is generally used in correlations estimating heat transfer coefficients:

$$r_{conv} = \frac{L}{\alpha \cdot Nu \cdot 2 \cdot LAI} \qquad (11)$$

Where α (m²/s) is the thermal diffusivity, and L is the characteristic dimension of the leaf for heat transfer. LAI is the *Leaf Area Index*, which expresses the ratio between (one-side) leaf area and the cultivated area. The $(2 \cdot LAI)$ correction factor expresses the ratio between the leaf surface area exchanging heat through convection (both faces of each leaf) and the cultivated area., This factor is necessary because $\dot{q}_{conv}$ is expressed in W/m² of cultivated area, but the actual heat transfer occurs over each face of each leaf. In other words, $(2 \cdot LAI)$ is the number of square meters of area exchanging heat by convection per square meter of cultivated area. It should be noted that some authors do not include the $(2 \cdot LAI)$ factor in r_a, in which case the factor appears directly in (9).

Longwave radiation

In greenhouses, plants can receive longwave radiation from heating systems such as pipes at a relatively high temperature. This incident radiation ($\dot{q}_{rad,lwh}$) can be considered as independent from the plant surface temperature, unlike the longwave exchange with other surfaces such as the greenhouse floor and ceiling ($\dot{q}_{rad,lwx}$), so the two terms are treated separately:

$$\dot{q}_{rad,lw} = \dot{q}_{rad,lwh} + \dot{q}_{rad,lwx} \qquad (12)$$

In line with the "big leaf" model fundamental assumptions, the plants are treated as a large horizontal surface which exchanges longwave radiation with the greenhouse floor and the greenhouse ceiling (or a thermal curtain if present). All surfaces are treated as infinite parallel plates, which gives:

$$\dot{q}_{rad,lwx} = 4 \cdot \sigma \cdot CAC \cdot \begin{pmatrix} E_{floor} \cdot \left(T_s^4 - T_{floor}^4\right) \\ +E_{ceil} \cdot (T_s^4 - T_{ceil}^4) \end{pmatrix} \qquad (13)$$

Where σ is the Stefan-Boltzmann constant, T_s is the plant surface temperature (the leaves are assumed be infinitely thin, and to have the same surface temperature on both faces), T_{floor} and T_{ceil} are respectively the floor and ceiling surface temperatures, and E_{floor} and E_{ceil} are the effective emittance for radiative heat transfer:

$$E_{\substack{floor \\ ceil}}^{-1} = \left(\varepsilon_p^{-1} + \varepsilon_{\substack{floor \\ ceil}}^{-1} - 1\right)^{-1} \qquad (14)$$

Where ε_p, ε_{floor}, and ε_{ceil} are the longwave emittance values for the plants, the floor, and the ceiling respectively.

The CAC factor in (13) is introduced because $\dot{q}_{rad,lwx}$ is expressed per unit area of cultivated area, while longwave heat transfer is assumed to occur from a surface equivalent to the horizontal projection of the leaf area. CAC was introduced in (7) and is discussed in more details above.

Latent heat exchange – plant transpiration

The driving potential for water vapor transfer is the difference between the water vapor concentration at the leaf surface (χ_s) and the water vapor concentration in the ambient air (χ), where both concentrations are expressed as densities in kg of water per m³ of humid air (χ is sometimes referred to as "absolute humidity", but should not be confused with the humidity ratio ω, in kg of water per kg of humid air). The air at the leaf surface is assumed to be

saturated, so that χ_s corresponds to saturation conditions at the surface temperature T_s, $\chi_s = \chi_{sat}(T_s)$. The resistance to water transfer by transpiration is the sum the leaf stomatal resistance (r_s) and the boundary layer resistance to vapor diffusion (r_v), both expressed in s m^{-1}. r_s can be seen as an "internal" resistance to vapor diffusion, while r_v can be seen as an "external" resistance to vapor diffusion (Stanghellini, 1987). The latent heat transfer associated with transpiration ($\dot{q}_{lat}$, W/m²) is the product of the mass flux (kg m^{-2} s^{-1}) and the latent heat of vaporization of water ($\mathcal{L}$, J kg^{-1}), which gives a similar equation to the one obtained for convection heat transfer:

$$\dot{q}_{lat} = \frac{\mathcal{L}}{(r_s + r_v)} \cdot (\chi_{sat}(T_s) - \chi) \qquad (15)$$

The "external" resistance r_v can be expressed as a function of the Sherwood number:

$$r_v = \frac{L}{\alpha \cdot Sh \cdot 2 \cdot LAI} \qquad (16)$$

Again, the $(2 \cdot LAI)$ factor expresses the ratio between the surface area from which vapor diffusion occurs and the cultivated area. In typical greenhouse operation conditions, the boundary layer resistance to water vapor transfer r_v is approximatively equal to the resistance to convective heat transfer r_{conv}, and that assumption is sometimes implied in plant models.

The "internal" (stomatal) resistance r_s similarly accounts for the resistance to vapor diffusion from the total leaf area (counting both faces) present above one square meter of cultivated area. If transpiration was uniform from both faces of all leaves, r_s would have the value of the stomatal resistance of a single leave divided by $(2 \cdot LAI)$. But many plant species have different stomatal resistance on upper and lower faces, so care should be exercised when parametrizing the proposed model with stomatal resistance values from the literature.

The stomatal resistance r_s depends on environmental factors and on the plant surface temperature. Jarvis (1976) proposed the assumption that the impact of different factors are independent, and that r_s can be expressed as a function of its minimal value $r_{s,min}$:

$$r_s = r_{s,min} \cdot f_1(\dot{q}_{rad,sw}) \cdot f_2(T_s) \cdot f_3(c_{CO_2}) \cdot f_4(VPD) \qquad (17)$$

Where VPD is the vapor pressure deficit, $p_{v,sat}(T_a) - p_v$, and c_{CO_2} is the CO_2 concentration. Various forms have been proposed for the correction functions. The proposed model implements the following corrections (Stanghellini, 1987):

$$f_1(\dot{q}_{rad,sw}) = \frac{\overline{\dot{q}_{rad,sw}} + 4.30}{\overline{\dot{q}_{rad,sw}} + 0.54} \qquad (18)$$

$$\mathrm{f_2(T_s)} = 1 + 0.023 \cdot (\mathrm{T_s} - 24.5) \qquad (19)$$

$$f_3(c_{CO_2}) = 1 + 6.1 \cdot 10^{-7} \cdot (c_{CO_2} - 200)^2 \qquad (20)$$

$$\mathrm{f_4(VPD)} = 1 + 4.3 \cdot \mathrm{VPD}^2 \qquad (21)$$

It is important to note that $\overline{\dot{q}_{rad,sw}}$ is the mean flux density per unit area (Stanghellini, 1987):

$$\overline{\dot{q}_{rad,sw}} = \frac{\alpha_s \cdot \dot{q}_{rad,sw}}{2 \cdot LAI} \qquad (22)$$

Solving the steady state heat balance

The proposed "plant model" consists in solve simultaneously (7) for $\dot{q}_{rad,sw}$, (10) for $\dot{q}_{conv}$, (15) for $\dot{q}_{lat}$, and (12) for $\dot{q}_{rad,lw}$ while using (6) to ensure that the energy balance is verified. Since T_s (which is unknown) appears in all terms of the heat balance as part of non-linear equations, an iterative approach is required. In the seminal work by Penman and Monteith, several approximations were made to linearize and simplify the equations to remove T_s from the heat balance terms, and these approximations are still widely used. However, these simplifications do not address, for example, the variation of r_s (or any other parameter) with T_s, and the treatment of non-symmetrical leaves (e.g. leaves with stomata on one side only) and the treatment of longwave radiation in methods derived from the Penman-Monteith equation are often unclear or erroneous (Schymanski and Or, 2017). Perhaps more importantly, the computing cost of solving a small number of non-linear equations simultaneously is very small in the context of a BPS tool such as TRNSYS, so an iterative method was selected. The developed model uses a secant method to solve the hygrothermal heat balance equations.

Figure 4 shows the data exchange between the "plant" component and the building model (Type 56) in TRNSYS.

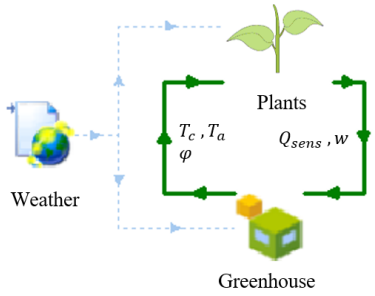

Figure 4: Data exchange between the developed plant component model TRNSYS Type 56

φ is the relative humidity in the greenhouse, other symbols have been described above.

Results

Results obtained from the proposed plant model were compared to other models to assess its validity. Systematic tests are not shown here due to lack of space, but the tests showed that, when parametrized carefully to ensure that resistance values and reference areas are the same, the

proposed model provides similar results to published results (e.g. Graamans *et al.*, 2017).

Additionally, the calculated leaf temperature was compared to measured data in a greenhouse in St-Damase, QC. The leaf temperature was measured with the multispectral infrared camera MS M350 from Telops on October 13, 2021. Figure 5 shows the processed image obtained from above the tomato rows (the top part of the image shows air circulation fans and fly traps hanging from the ceiling).

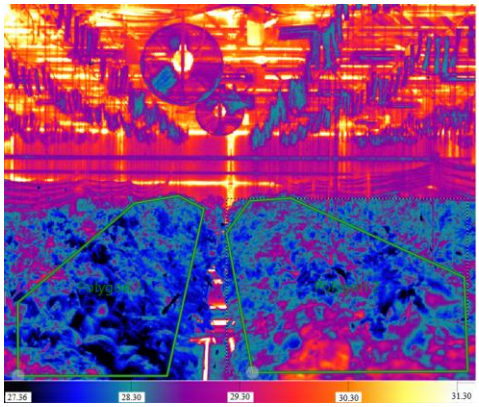

Figure 5: Infrared image of mature tomato plants

The other parameter which was measured on site was the *LAI* of the tomato plants. As shown by Figure 6, leaves were photographed with a millimetric paper in the background, the image was digitized and then the Digimizer program was used to calculate the leaf area.

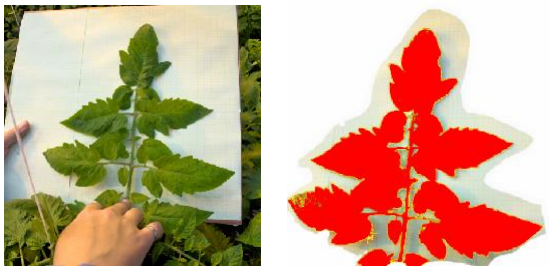

Figure 6: First and third step done to measure the LAI

Knowing that plants are trimmed to leave 15 leaves per tomato plant in this greenhouse, it was possible to calculate the total leaf area of the greenhouse considering that there are 2.4 plants/m^2. Finally, the *LAI* was calculated with its definition:

$$LAI = \frac{\text{(single side) leaf area}}{\text{cultivated area}} \qquad (23)$$

Several temperature measurements were taken that day, but only two are presented here: one shaded leaf of a tomato plant, and the unshaded leaves of two rows of tomato plants in the commercial greenhouse (shown in Figure 5). Table 3 shows the results.

Table 3: Measured data at the commercial greenhouse

Data set	Measured average temp. [°C]	Solar radiation [W/m^2]	Net absorbed radiation (*) [W/m^2]
Shaded leaves	24.4	409	160.3
Unshaded leaves	28.2	441	167.4

(*) The net radiation absorbed was not measured but calculated with equation (7).

Table 4 shows other parameters (environmental conditions and plant parameters) in the greenhouse.

Table 4: Greenhouse parameters on October 13, 2021

Parameter	Value	Unit
T_a	24.7	°C
Relative humidity	75	%
$d^{(*)}$	0.05	m
LAI	1.6	-
CAC	0.8	-
$\varepsilon^{(*)}$	0.98	-

(*) The characteristic length and the emissivity of the plant were not measured but taken from the literature (Katsoulas and Stanghellini, 2019; López *et al.*, 2012)

Figure 7 shows the comparison between the two measured leaf temperatures (black dots) and the model for the specified parameters (red dot). The model represents the average temperature for all leaves, which is located between the measured values for unshaded and shaded leaves. The figure also shows the model response when the net absorbed radiation varies from 0 to 400 W m^{-2} (red line). Finally, the empirical model proposed by Wei et al. (2021) is plotted (grey line) as a comparison. The air temperature is represented by the dotted black line.

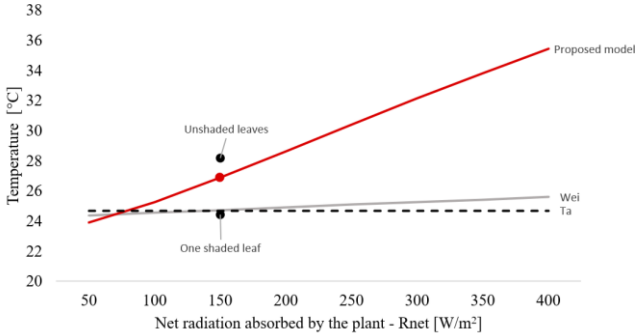

Figure 7: leaf temperature comparison

The Wei *et al.* (2021) model seems to represent a temperature closer to shaded leaves, with a small dependency on absorbed radiation.

Application: full greenhouse model

To demonstrate the usefulness of the new TRNSYS components to model plants and surface condensation, some results are presented in this section for a typical greenhouse in the Quebec context (Pelletier and Godbout, 2017). The greenhouse contains 5 identical bays. The north wall and the lower part of other walls are opaque and insulated, while all other surfaces are made of transparent cover on a metallic structure. Figure 8 presents the typical greenhouse, and

Table 5 gives some information about materials and U-values. Figure 9 shows the complete model in TRNSYS.

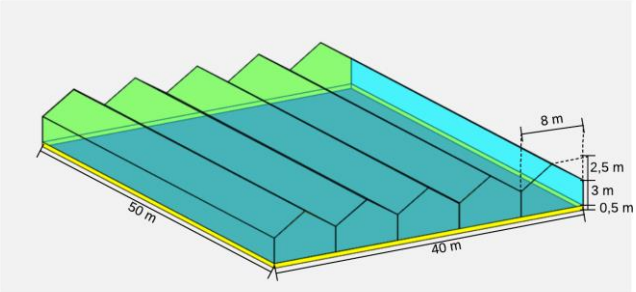

Figure 8: Typical greenhouse

The materials used in the model for each part of the greenhouse is shown in the table below with their corresponding U factor. A constant infiltration rate is modelled, equal to 3 volumes per hour.

Table 5: Selected construction details

	Materials	U-value [W/m²-K]
Transparent cover	Double polyethylene	4.0
North wall	Concrete & polystyrene	0.40
Other opaque walls	Polystyrene	0.45

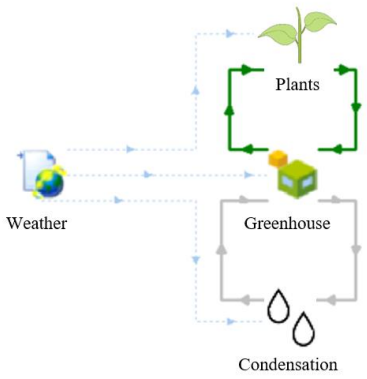

Figure 9: Full greenhouse model in TRNSYS

Changes to Type 56 parameters

In our model, plants are not present as "surfaces" in the Type 56. They are represented by latent gains, and net radiative transfer to the ceiling and floor are represented by "wall gains" (surface gains). To avoid "double counting" incident solar gains, the part of solar gains which is absorbed by plants should be removed from the zone. At this stage, this is achieved by artificially reducing the solar absorptance of the floor by a factor $(1 - CAC)$. Similarly, there is no obstacle to longwave radiation exchange between the floor and the ceiling in Type 56, while in reality most radiation will be exchanged with the plants, so their emittance value is artificially reduced by the same factor.

Results

The results of the global greenhouse model are illustrated by presenting the plant transpiration and water condensation on surfaces, as well as the relative humidity inside the greenhouse. Figure 10 shows the hygrothermal exchanges on a cold and sunny winter day. Transpiration increases significantly during the sunlit hours, so the relative humidity increases to close to 80 %, even though condensation is high. During the night, condensation represents about half of the transpiration, and the humidity remains relatively constant around 40 %, thanks to infiltration.

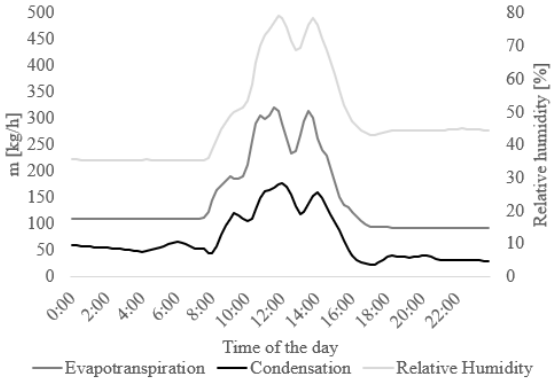

Figure 10: Transpiration and condensation on a cold day

Figure 11 shows them for a warm summer day. Transpiration during the day is much larger than in winter (around double), and the indoor humidity is very high. Very little condensation occurs at the end of the night, when surface temperatures are the lowest. It should be noted that the current model does not represent ventilation openings that could be used to keep indoor humidity lower. The simulated relative humidity is unrealistically high, as greenhouse control systems would likely use natural ventilation (and possibly heating) to reduce indoor humidity.

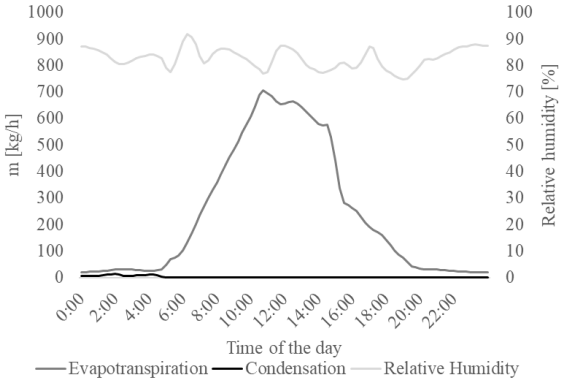

Figure 11: Transpiration and condensation on a warm day

Conclusion

This paper has presented two new TRNSYS component models representing condensation and the hygrothermal balance of plants for greenhouse modelling.

Both component models have been compared to published or original experimental data to check their validity in selected operating conditions. The application to a typical greenhouse in the Quebec context shows that the two components can be used in combination with the multizone model known as Type 56 to represent the hygrothermal processes in greenhouses.

Further work will address modelling of infiltration (or natural ventilation) with controllable vent openings, thermal screens between the greenhouse and the roof, detailed modelling of heating systems, and artificial lighting.

Acknowledgement

The authors would like to thank Etienne Robert at Polytechnique Montréal for his help with the infrared camera and Rosaire Sauriol from *Excel Serres* who allowed us to take measures in the commercial greenhouse.

References

Bouthillette Parizeau (2021) *Étude et proposition de solutions visant la récupération de chaleur d'un centre de données vers une serre*. Montréal, QC, CAN: Hydro-Québec, p. 163.

Gouvernement du Québec (2020) *Croissances des serres au Québec, Site officiel du gouvernement du Québec*.

Graamans, L. *et al.* (2017) 'Plant factories; crop transpiration and energy balance', *Agricultural Systems*, 153, pp. 138–147. doi:https://doi.org/10.1016/j.agsy.2017.01.003.

Griffith, P. (1983) 'Dropwise condensation(mechanism and heat transfer coefficients correlation and prediction)', *Handbook of heat transfer.(A 74-17085 05-33) New York, McGraw-Hill Book Co., 1973*, pp. 12–34.

Jarvis, P.G. (1976) 'The interpretation of the variations in leaf water potential and stomatal conductance found in canopies in the field', *Philosophical Transactions of the Royal Society of London. B, Biological Sciences*, 273(927), pp. 593–610. doi:10.1098/rstb.1976.0035.

Katsoulas, N. and Stanghellini, C. (2019) 'Modelling Crop Transpiration in Greenhouses: Different Models for Different Applications', *Agronomy*, 9(7), p. 392. doi:10.3390/agronomy9070392.

Klein, S.A. *et al.* (2021) *TRNSYS 18 – A TRaNsient SYstem Simulation program, User manual. Version 18.4*. Madison, WI: University of Wisconsin-Madison.

López, A. *et al.* (2012) 'Determining the emissivity of the leaves of nine horticultural crops by means of infrared thermography', *Scientia Horticulturae*, 137, pp. 49–58. doi:10.1016/j.scienta.2012.01.022.

Mohammadi, B., Ranjbar, S.F. and Ajabshirchi, Y. (2021) 'Comprehensive evaluation of a semi-solar greenhouse: energy, exergy and economic analyses with experimental validation', *Scientia Iranica*, 0(0), pp. 0–0. doi:10.24200/sci.2021.53709.3375.

Monteith, J.L. (1965) 'Evaporation and environment', *Symposia of the Society for Experimental Biology*, 19, pp. 205–234.

Monteith, J.L. and Unsworth, M.H. (2013) *Principles of environmental physics: plants, animals, and the atmosphere*. 4th ed. Amsterdam ; Boston: Elsevier/Academic Press.

Nguyen, C.-K. *et al.* (2019) 'A full-scale experimental study concerning the moisture condensation on building glazing surface', *Building and Environment*, 156, pp. 215–224. doi:https://doi.org/10.1016/j.buildenv.2019.04.024.

Pelletier, F. and Godbout, S. (2017) *Consommation d'énergie et émissions de gaz à effet de serre en production serricole au Québec*. 400023. Longueuil, Québec, Canada.

Schymanski, S.J. and Or, D. (2017) 'Leaf-scale experiments reveal an important omission in the Penman–Monteith equation', *Hydrology and Earth System Sciences*, 21(2), pp. 685–706. doi:10.5194/hess-21-685-2017.

Stanghellini, C. (1987) *Transpiration of greenhouse crops: an aid to climate management*. phd. Wageningen University.

Talbot, M.-H. and Monfet, D. (2020) 'Estimating the impact of crops on peak loads of a Building-Integrated Agriculture space', *Science and Technology for the Built Environment*, 26(10), pp. 1448–1460. doi:10.1080/23744731.2020.1806594.

Ward, R. *et al.* (2015) 'Simulation of plants in buildings; incorporating plant-Air interactions in building energy simulation', in. *In Proceedings of BS2015: 14th Conference of International Building Performance Simulation Associatio*, pp. 2256–2263.

Ward, R.M. and Choudhary, R. (2014) 'A bottom-up energy analysis across a diverse urban building portfolio: retrofits for the buildings at the Royal Botanic Gardens, Kew, UK', *Building and Environment*, 74, pp. 132–148. doi:10.1016/j.buildenv.2013.12.018.

Wei, A., Nourozi, B. and Chen, Y. (2021) 'Incorporating Plants Modelling in Greenhouse Design', in *Proceedings of eSim 2020: the 11th conference of IBPSA-Canada*. *eSim 2020*, Vancouver, BC, CAN.